Click to view Poster version of this presentation

Investigation and Identification of Pyrolysis Attributes that Can Assist in Predicting Producible Hydrocarbon in the Unconventional Eagle Ford Formation*

Albert Maende[1], Brian Horsfield[2], Sascha Kuske[2], Brian Jarvie[3], Dan Jarvie[1], and W. David Weldon[1]

Search and Discovery Article #80733 (2020)**
Posted October 26, 2020

*Adapted from oral presentation accepted for the 2020 AAPG Annual Convention and Exhibition online meeting, September 29 – October 1, 2020
 DOI:10.1306/80733Maende2020

[1]Wildcat Technologies, LLC, Humble, TX, USA (albertmaende@wildcattechnologies.com)
[2]German Research Centre for Geosciences (GFZ), Potsdam, Germany
[3]GeoMark Research Lab, Ltd, Humble, TX, USA

Abstract

Prediction of producible hydrocarbons in unconventional formations, is vital because it governs returns on investments. Kuske et al., 2019 used a PhaseSnapShot workflow to model target well hydrocarbon phases based on PVT data and nearest slightly less mature well. Gorynski et al., 2019, showed low-maturity shales can be dominated by heavy (C_{32+}) oils and that the ratios of SARA components in the C_{15+} fraction of produced fluid and core extract can be used to estimate the mobile oil. Pepper et al., 2019 discriminated fluid saturation from sorbed oil.

Prediction of producible hydrocarbons in unconventional formations is complicated by the co-occurrence of sorbed oil with fluid saturation. Our objective was to investigate and identify pyrolysis attributes that can assist in predicting producible hydrocarbon in unconventional formations. Seven core samples spanning the Eagle Ford Formation’s early mature, oil window and condensate/wet gas zones were analyzed on the HAWK pyrolysis instrument using both classical bulk-flow pyrolysis and HAWK-PAM the latter of which provides insights into boiling ranges. Hydrocarbons were extracted using DCM, while the extracted rock was analyzed using both pyrolysis methods. The extract was quantified and fingerprinted using both gas chromatography and PAM. The suppression effect of ‘S2 shoulders’ on maturity was evident on four cores.

While the S1 mg HC/g rock values for the seven core samples were 5.3, 2.23, 2.82, 2.19, 8.33, 6.68, and 3.94 for Tmax (°C) maturity values of 436, 442, 458, 465, 443, 434, and 435 respectively, their S1+ ($S2_{\text{whole rock}}$ - $S2_{\text{extract rock}}$) values were 20.07, 5.13, 5.18, 3.41, 15.32, 25.6, and 12.54 mg HC/g rock respectively. These two measurements, however, do not enable the discrimination of producible hydrocarbons because of the presence of sorbed oil which is highest in early mature cores.

Conversion of mg HC/g rock measurements to their respective organic carbon using the assumption that 85% of hydrocarbons content is organic carbon, together with conversion of the quantified extracted organic matter (EOM) from ppm to weight % enabled the identification of a new set of pyrolysis attributes: For the Tmax (°C) maturity values of 436, 442, 458, 465, 443, 434, and 435 respectively, S1 organic Carbon/EOM was 0.18, 0.27, 0.34, 0.3, 0.42, 0.18, and 0.23: The (C_4 - C_{19})/EOM ratio was 0.05, 0.1, 0.14, 0.14, 0.17, 0.05, and 0.09 while that of (C_4 - C_{36})/EOM was 0.31, 0.36, 0.5, 0.39, 0.55, 0.24, and O.34 respectively. The ratio of (C_4 - C_{19})/(C_4 - C_{36}) yielded values of 0.17, 0.27, 0.28, 0.37, 0.31, 0.22, and 0.25. These four pyrolysis attributes enable ranking of predicted producible hydrocarbons, with the highest to lowest values in each of the attributes, corresponding to highest to lowest producible hydrocarbon contents. Determination of these pyrolysis attributes for a producing interval can provide calibration for predicting similar production.

References Cited

EIA, 2014, Updates to the EIA Eagle Ford Play Maps, https://www.eia.gov/maps/pdf/eagleford1014.pdf. Website accessed October 2020.

Gorynski, K.E., M.H. Tobey, D.A. Enriquez, T.M. Smagala, J.L. Dreger, and R.E. Newhart, 2019, Quantification and Characterization of Hydrocarbon-Filled Porosity in Oil-Rich Shales Using Integrated Thermal Extraction, Pyrolysis and Solvent Extraction: American Association of Petroleum Geologists Bulletin, v. 103/3 p. 723-744.

Jarvie, D.M., B.M. Jarvie, W.D. Weldon, and A. Maende, 2015, Geochemical Assessment of in situ Petroleum in Unconventional Resource Systems: Unconventional Resources Technology Conference, San Antonio, Texas, USA, 20-22 July 2015, Unconventional Resources Technology Conference (URTeC 2173379), p. 875-894. doi.org/10.15530/urtec-2015-2173379

Jarvie, D.M., 2012, Shale Resource Systems for Oil and Gas: Part 2 – Shale Oil Resource Systems, *in* J.A. Breyer (ed.), Shale Reservoirs – Giant Resources for the 21st Century: American Association of Petroleum Geologists Memoir 97, p. 89-119.

Kuske, S., B. Horsfield, J. Jweda, G.E. Michael, and Y. Song, 2019, Geochemical Factors Controlling the Phase Behavior of Eagle Ford Shale Petroleum Fluids: American Association of Petroleum Geologists Bulletin, v. 103/4, p. 835-870.

Maende, A., A. Pepper, D.M. Jarvie, and W.D. Weldon, 2017, Advanced Pyrolysis Data and Interpretation Methods to Identify Unconventional Reservoir Sweet Spots in Fluid Phase Saturation and Fluid Properties (API Gravity) From Drill Cuttings and Cores: AAPG 2017 Annual Convention and Exhibition, Houston, Texas, April 2-5, 2017, Search and Discovery Article #80596 (2017). Website accessed October 2020.

Ononogbu, U., 2012, Biomarkers: Review and Application to the Eagle Ford Formation: M.S. Thesis, University of Texas at Arlington, 60 p.

Pepper, A., S. Perry, and L. Heister, 2019, Saturation Isn't What It Used to Be: Towards More Realistic Petroleum Fluid Saturations and Produced Fluid Compositions in Organic-Rich Unconventional Reservoirs: Unconventional Resources Technology Conference held in Denver, Colorado, USA,22-24 July 2019, Unconventional Resources Technology Conference (URTeC 196), p. 2985-3000. doi:10.15530/urtec-2019-196

Investigation and Identification of Pyrolysis Attributes that can Assist in Predicting Producible Hydrocarbon in the Unconventional Eagle Ford Formation

Presented at: AAPG 2020 Annual Convention & Exhibition, Houston, Texas, USA, September 29th – October 1st by

Albert Maende[1], Brian Horsfield[2], Sascha Kuske[2], Brian Jarvie[3], Dan Jarvie[1], and W. David Weldon[1]
(1) Wildcat Technologies, Humble, TX, USA(albertmaende@wildcattechnologies.com), (2) German Research Centre for Geosciences (GFZ), Potsdam, Germany (3) Geomark Research Rock Lab, Humble, TX, USA

Talk Outline

- Objective and previous work
- Two current pyrolysis methods invoked in this study and their limitations
- New method for investigation for pyrolysis attributes
- Analyses of Eagle Ford Formation’s core and extracted core samples; Classical pyrolysis, HAWK-PAM, quantification of extractable organic matter and gas chromatography
- Results and Interpretation
- Graphical plots of selected pyrolysis parameters against maturity (Tmax)
- Pyrolysis parameters demarcation of immature, oil window and condensate/wet gas zones
- Comparison of pyrolysis and maturity measurements of cores and extracted cores
- Gas chromatography fingerprinting of the core extracts and evaporative loss determination
- Pyrolysis attributes of the Shale Prospectivity Tool
- Cut-off values of the Shale Prospectivity Tool for determination of producible oil zones
- Shale Prospectivity Tool mapping of the drilled structure
- Conclusions

Objective and Previous Work

Introduction

Seven core samples spanning the Eagle Ford Formation's early mature, oil window and condensate/wet gas zones (Figure 1 and Figure 2) were analyzed as whole rock, extracts and extracted rock, with the objective of investigating and identifying pyrolysis attributes that can assist in predicting producible hydrocarbons in unconventional formations.

This is a vital need because it governs returns on investments.

Kuske *et. al.*, 2019 used a PhaseSnapShot workflow to model target well hydrocarbon phases based on PVT data and nearest slightly less mature well.

Previous Work and Current Pyrolysis Methods

Gorynski *et. al.*, 2019, showed low-maturity shales can be dominated by heavy (C_{32+}) oils and that the ratios of SARA components in the C_{15+} fraction of produced fluid and core extract can be used to estimate the mobile oil.

Pepper *et.al.*, 2019 discriminated fluid saturation (producible hydrocarbons) from sorbed oil.

Prediction of producible hydrocarbons in unconventional formations is complicated by the co-occurrence of sorbed oil with fluid saturation.

The current pyrolysis methods that are invoked in this study are Classical Pyrolysis and HAWK-PAM

Classical Pyrolysis and HAWK-PAM

Classical Pyrolysis, are analyses to determine thermally released oil (S1 in mg HC/g rock) at 300 °C, hydrocarbons yield from pyrolysis of kerogen (S2 in mg HC/g rock) through heating in an inert environment using a ramp rate of 25 °C from 300 to 650 °C, pyrolysis measurements of both CO and CO_2 (S3CO in mg CO/g rock and S3CO2 in mg CO_2/g rock) and maturity (Tmax in °C) determined as the temperature at the maximum generation of hydrocarbons on the S2 peak.

HAWK-PAM, are analyses whereby, a ramp rate of 25°C was utilized to generate five petroleum peaks – four on oil fractions and one on kerogen. It is a pyrolysis method through which, determination of the occurrence of carbon number groupings corresponding to $C_4 – C_5$ (Oil-1) at ~50 – 100 °C, $C_6 – C_{10}$ (Oil-2) at 100 °C , $C_{11} – C_{19}$ (Oil-3) at 100 – 180 °C, $C_{20} – C_{36}$ (Oil-4) at 180 – 350 °C and C_{37+} (K-1; Kerogen plus any C_{37+}) at 350 – 650 °C, is done. In addition, maturity (K-1 Tmax in ° C) is determined as the temperature at the maximum generation of hydrocarbons on the K-1 peak (Maende *et. al*., 2017).

Albert Maende, Brian Horsfield, Sascha Kuske, Brian Jarvie, Dan Jarvie, and W. David Weldon

Statement of the Limitations of both Classical Pyrolysis and HAWK-PAM

Classical Pyrolysis and **HAWK-PAM** measurements, however, do not enable the discrimination of producible hydrocarbons because of the presence of sorbed oil which is highest in early mature cores.

New Method of Investigation for Pyrolysis Attributes

Conversion of mg HC/g rock measurements to their respective organic carbon using the assumption that 85% of hydrocarbons content in petroleum is organic carbon, together with conversion of the quantified extracted organic matter (EOM) from ppm to weight % enabled the identification of a new set of pyrolysis attributes, collectively referred to as the “Shale Prospectivity Tool”. Seven core samples from the Eagle Ford Formation were analyzed.

Albert Maende, Brian Horsfield, Sascha Kuske, Brian Jarvie, Dan Jarvie, and W. David Weldon

Location and Stratigraphy of Eagle Ford Shale Play

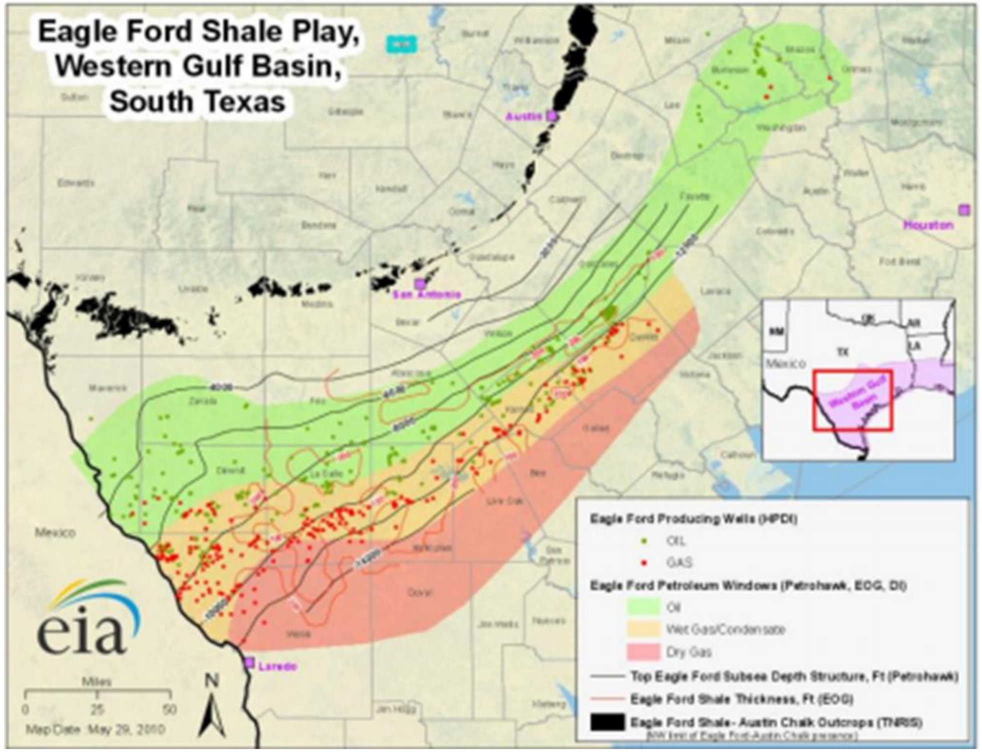

Figure 1. Eagle Ford Shale Play, Western Gulf Basin, South Texas (EIA, 2014)

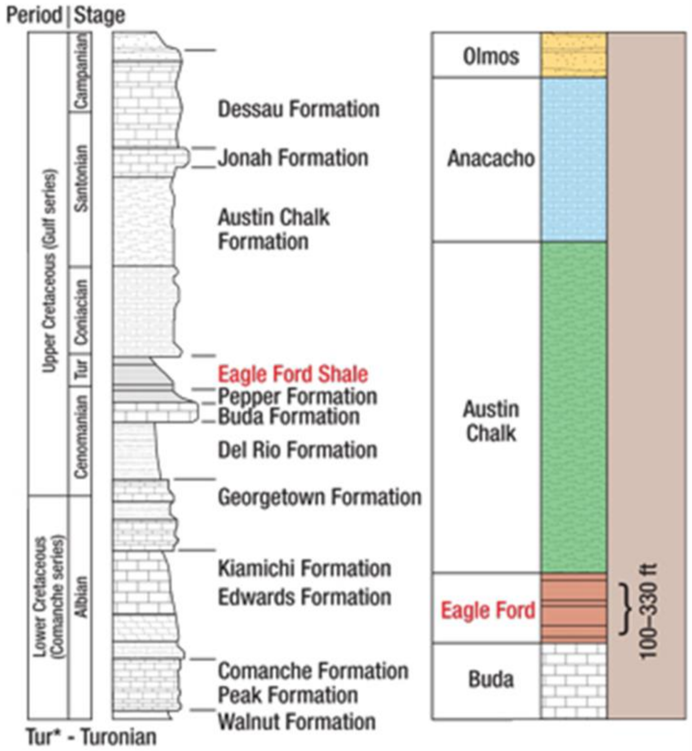

Figure 2. Stratigraphy of Western Gulf Basin, South Texas (Ononogbu, 2012)

Albert Maende, Brian Horsfield, Sascha Kuske, Brian Jarvie, Dan Jarvie, and W. David Weldon

Analyses

Analyses of core and extracted core samples from the Eagle Ford Formation

The seven core and extracted core samples from the Eagle Ford Formation were analyzed on the HAWK pyrolysis instrument using both classical bulk-flow pyrolysis and HAWK-PAM, the latter of which provides insights into boiling ranges.

Hydrocarbons were extracted using dichloromethane (DCM), while the extracted rock was analyzed using both pyrolysis methods. The extract was quantified and fingerprinted using gas chromatography and will later be quantified and fingerprinted using PAM.

HAWK® Pyrolysis

The seven core and extracted core samples were analyzed on the HAWK Pyrolysis, TOC & Carbonate Carbon instrument using two pyrolysis methods, namely; Classical Pyrolysis and HAWK-PAM.

Extractable Organic Matter

Extractable Organic Matter (EOM)

Quantitative extraction of extracts for Gas Chromatography analyses was done using the Dionex ASE 350 model.

For Dionex extraction, the rock sample is ground to 60 mesh size, after which a weight of sample ranging from 5 to 20 grams is placed into the Dionex’ steel extraction cell and then using dichloromethane as the solvent, extraction of the oil is done within the 40 °C to 100 °C operating temperature range of the Dionex.

The extract is then dried under a fume hood and weighed for quantification.

Gas Chromatography (GC)

Gas Chromatography (GC)

Whole Oil Gas Chromatography on the extracted oil was performed using an Agilent GC. Petroleum extracted from rock samples can be fingerprinted by gas chromatography (GC).

A fingerprint of petroleum provides an indication of the distribution and yield of resolvable compounds, i.e., basically a histogram of the individual compounds that can be separated by this analytical technique.

An oil or extract with an internal standard(s) is injected into a GC inlet which vaporizes the petroleum in the presence of an inert carrier gas onto a capillary column that may range from 10 to 150 meters in length.

Gas Chromatography (GC)

The internal surface of the column is coated with a chemical phase utilized for the required analytical need.

This chemical phase interacts with the hydrocarbon molecules moving through the length of the column resulting in separation of the alkanes as well as many iso-alkanes, cyclo-alkanes, and some aromatic hydrocarbons.

The end of the column passes the effluent into a flame ionization detector (FID).

Integration of the fingerprint provides the weight or mole percent of each compound relative to the internal standard(s) and is used to characterize the alkane fraction of the petroleum (Jarvie, 2015).

Results and Interpretation

Classical Pyrolysis, HAWK-PAM, Extractable Organic Matter (EOM) & Gas Chromatography (GC)

Table 1. Classical Pyrolysis, HAWK-PAM and Extractable Organic Matter

Sample ID	Method	Sample Type	S1 (mg HC/g rock)	S2 (mg HC/g rock)	S3 (mg CO2/g rock)	Tmax (°C)	Production Index (S1/S1 + S2)	Sum(S1 + S2) mg HC/g rock	Extractable Organic Matter (EOM) (ppm)	$S1_{whrk}$ - $S1_{extrk}$ + $S2_{whrk}$ - $S2_{extrk}$ (Jarvie, 2012)
G014171	Classical Pyrolysis	Core	5.30	25.55	0.48	436	0.17	30.85	24817	19.91
G014174	Classical Pyrolysis	Core	2.23	12.17	0.34	442	0.15	14.40	7015	4.93
G014177	Classical Pyrolysis	Core	2.82	5.46	0.24	458	0.34	8.28	6955	4.95
G014180	Classical Pyrolysis	Core	2.19	2.91	0.29	465	0.43	5.10	6174	3.16
G014183	Classical Pyrolysis	Core	8.33	11.99	0.41	443	0.41	20.32	16943	15.01
G014185	Classical Pyrolysis	Core	6.68	58.08	0.45	434	0.1	64.76	30933	25.47
G014188	Classical Pyrolysis	Core	3.94	52.47	0.42	435	0.07	56.41	14700	12.41
G014171	Classical Pyrolysis	Extracted Core	0.16	10.78	0.27	440	0.01	10.94		
G014174	Classical Pyrolysis	Extracted Core	0.20	9.27	0.30	443	0.02	9.47		
G014177	Classical Pyrolysis	Extracted Core	0.23	3.10	0.31	465	0.07	3.33		
G014180	Classical Pyrolysis	Extracted Core	0.25	1.69	0.26	476	0.13	1.94		
G014183	Classical Pyrolysis	Extracted Core	0.31	5.00	0.42	458	0.06	5.31		
G014185	Classical Pyrolysis	Extracted Core	0.13	39.16	0.31	440	0.00	39.29		
G014188	Classical Pyrolysis	Extracted Core	0.13	43.87	0.25	437	0.00	44.00		

Sample ID	Method	Sample Type	Oil-1 (mg HC/g rock) (C_4 - C_5)	Oil-2 (mg HC/g rock) (C_6 - C_{10})	Oil-3 (mg HC/g rock) (C_{11} - C_{19})	Oil-4 (mg HC/g rock) (C_{20} - C_{36})	K-1 (mg HC/g rock) (Kerogen plus any C_{37+})	K-1 Tmax (°C)	Sum(Oil-1, Oil-2 & Oil-3) mg HC/g rock	Sum(Oil-1, Oil-2, Oil-3 & Oil-4) mg HC/g rock	Sum(Oil-1, Oil-2, Oil-3, Oil-4 & K-1) mg HC/g rock	Whole Core Sum(Oil-1, Oil-2, Oil-3, Oil-4 & K-1) - Ext Core Sum(Oil-1, Oil-2, Oil-3, Oil-4 & K-1) mg HC/g rock	Mobility Index; Sum(Oil-1, Oil-2 & Oil-3)/Sum(Oil-1, Oil-2, Oil-3 & Oil-4) (Sum of C_4 - C_{19}/Sum of C_4 - C_{36})	S2 - K1 (mg HC/g rock)	Sum (Oil-1, Oil-2, Oil-3 & Oil-4) - S1 (mg HC/g rock)
G014171	HAWK-PAM	Core	0	0.07	1.47	7.43	23.32	436	1.54	8.97	32.29	20.33	0.17	2.23	3.67
G014174	HAWK-PAM	Core	0	0.04	0.78	2.19	11.47	442	0.82	3.01	14.48	5.42	0.27	0.70	0.78
G014177	HAWK-PAM	Core	0	0.07	1.06	2.93	5.11	456	1.13	4.06	9.17	5.49	0.28	0.35	1.24
G014180	HAWK-PAM	Core	0	0.11	0.93	1.8	2.6	464	1.04	2.84	5.44	3.35	0.37	0.31	0.65
G014183	HAWK-PAM	Core	0.02	0.37	3.04	7.61	9.54	443	3.43	11.04	20.58	15.33	0.31	2.45	2.71
G014185	HAWK-PAM	Core	0	0.2	1.7	6.92	57.9	436	1.9	8.82	66.72	27.56	0.22	0.18	2.14
G014188	HAWK-PAM	Core	0.01	0.23	1.25	4.44	52.2	435	1.49	5.93	58.13	12.84	0.25	0.27	1.99
G014171	HAWK-PAM	Extracted Core	0	0	0.07	0.23	11.66	439	0.07	0.3	11.96				
G014174	HAWK-PAM	Extracted Core	0	0	0.07	0.18	8.81	443	0.07	0.25	9.06				
G014177	HAWK-PAM	Extracted Core	0	0	0.07	0.27	3.34	463	0.07	0.34	3.68				
G014180	HAWK-PAM	Extracted Core	0	0.01	0.12	0.2	1.76	475	0.13	0.33	2.09				
G014183	HAWK-PAM	Extracted Core	0	0.01	0.1	0.26	4.88	457	0.11	0.37	5.25				
G014185	HAWK-PAM	Extracted Core	0	0	0.05	0.38	38.73	439	0.05	0.43	39.16				
G014188	HAWK-PAM	Extracted Core	0	0	0.03	0.27	44.99	436	0.03	0.3	45.29				

The suppression effect of ‘S2 shoulders’ on maturity was evident on four cores (those of Tmax 436, 458, 465 and 443). The “S2 shoulder” which is an overlap of the heavier oil component from S1 into S2 is quantifiable through the almost equality of the “S2 – K1” value with the “Sum(Oil-1, Oil-2, Oil-3 and Oil-4 – S1” value of the cores of Tmax 442 and 443 which are of mid oil window maturity (Table 1).

Albert Maende, Brian Horsfield, Sascha Kuske, Brian Jarvie, Dan Jarvie, and W. David Weldon

Graphical Plots of Selected Pyrolysis Measurements against Maturity (Tmax)

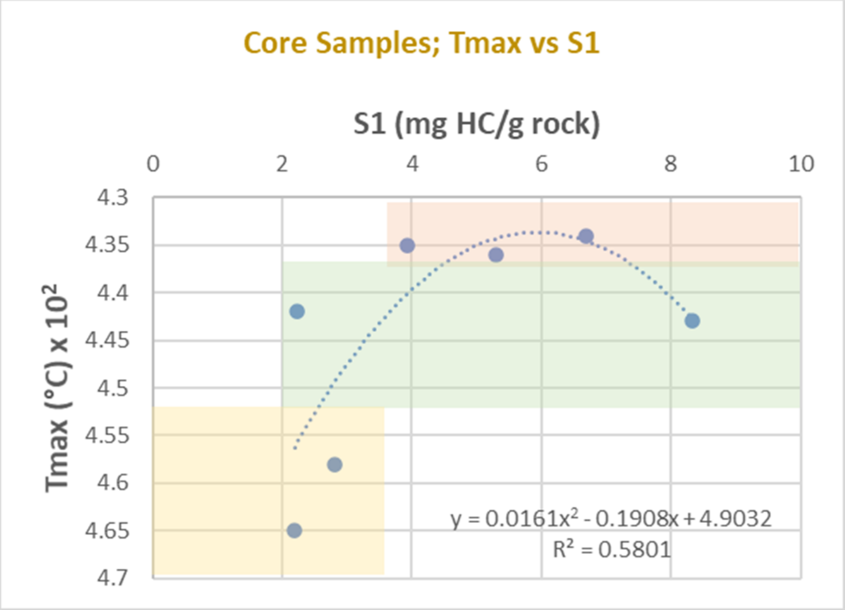

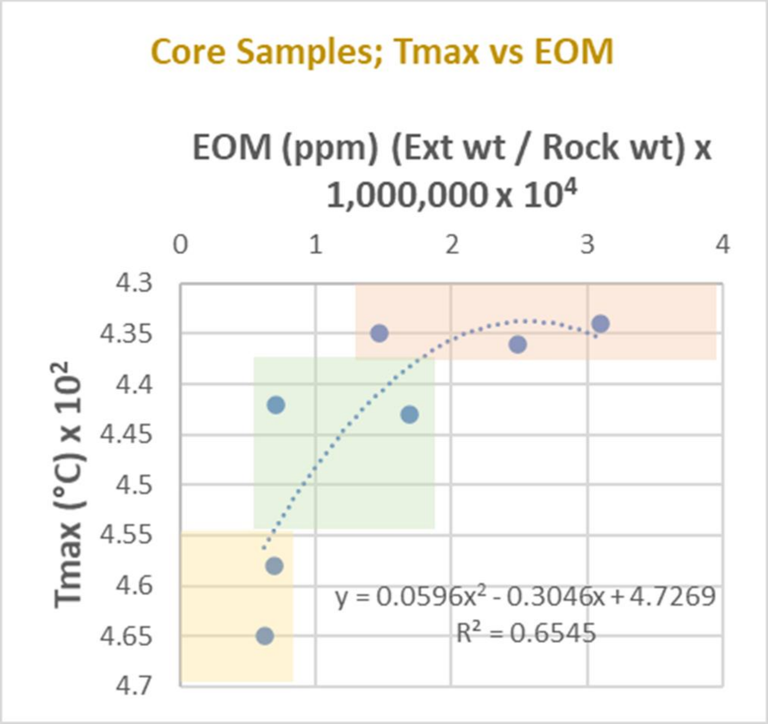

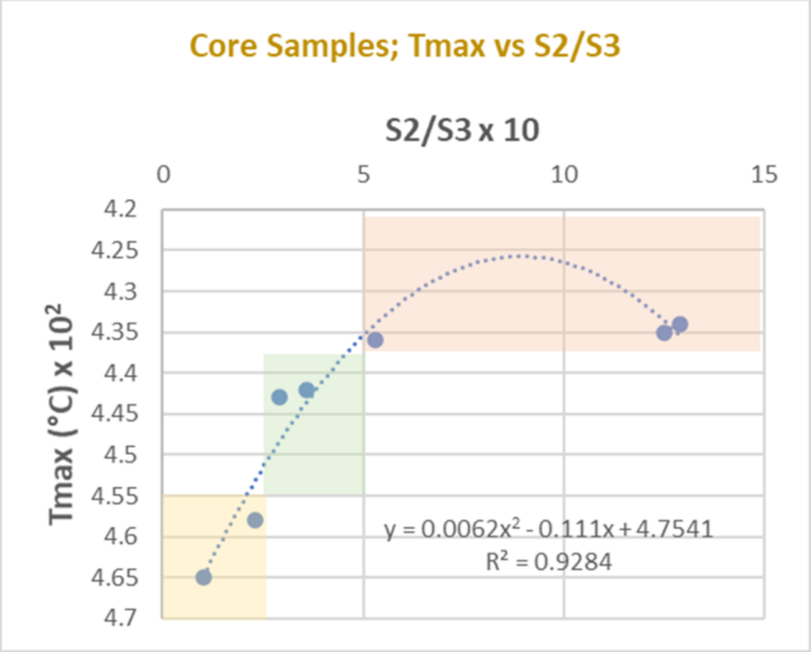

Immature
Oil Window
Condensate to Wet Gas

Albert Maende, Brian Horsfield, Sascha Kuske, Brian Jarvie, Dan Jarvie, and W. David Weldon

Graphical Plots of Selected Pyrolysis Measurements against Maturity (Tmax)

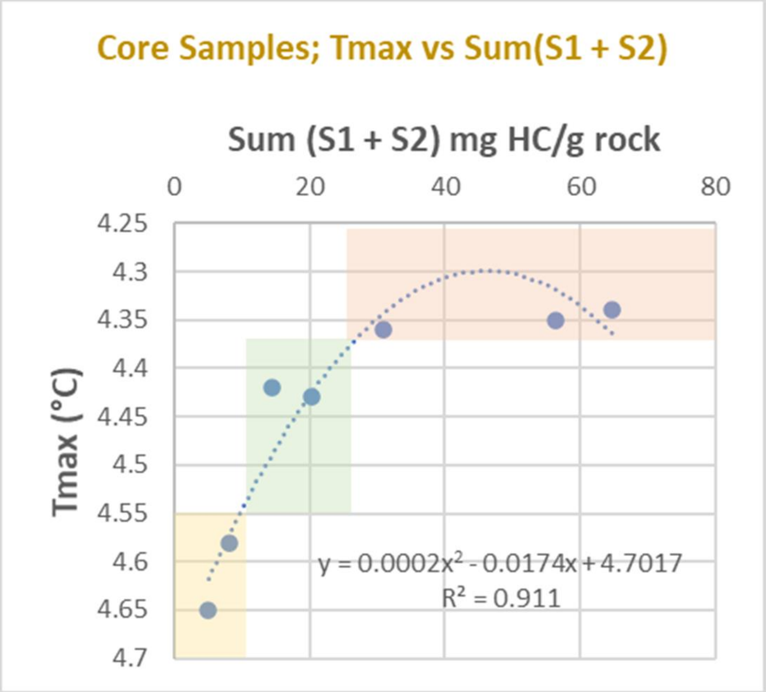

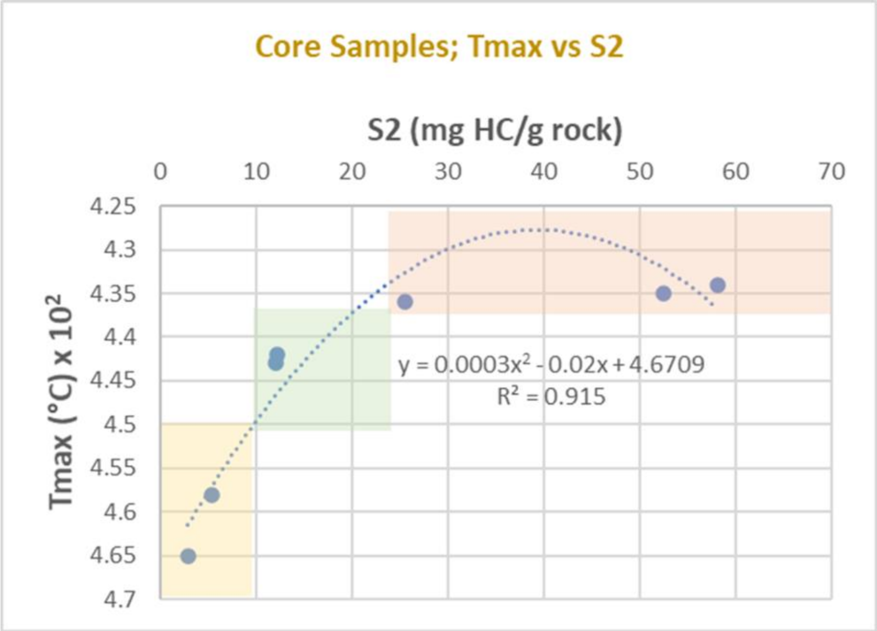

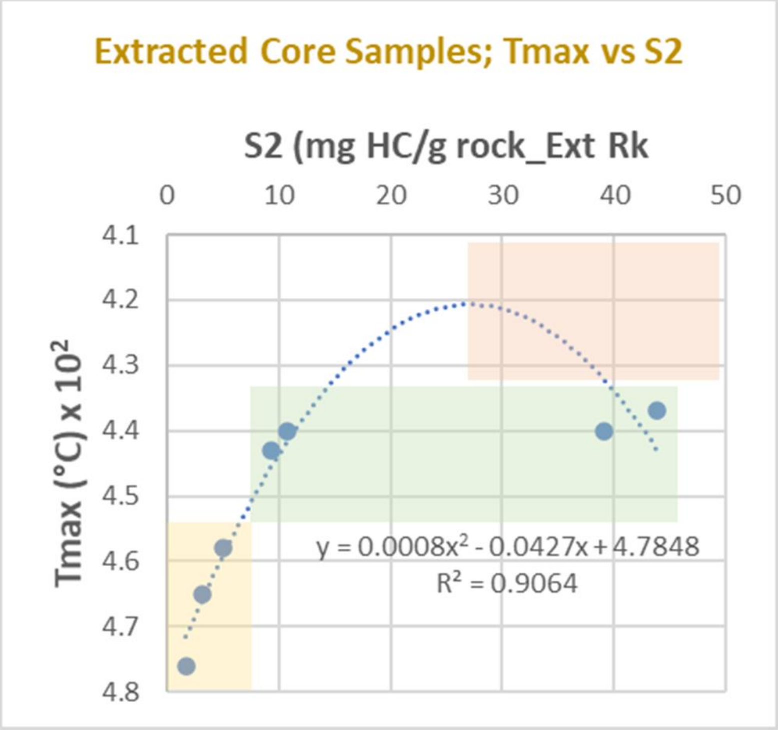

Immature
Oil Window
Condensate to Wet Gas

Albert Maende, Brian Horsfield, Sascha Kuske, Brian Jarvie, Dan Jarvie, and W. David Weldon

Graphical Plots of Selected Pyrolysis Measurements against Maturity (Tmax)

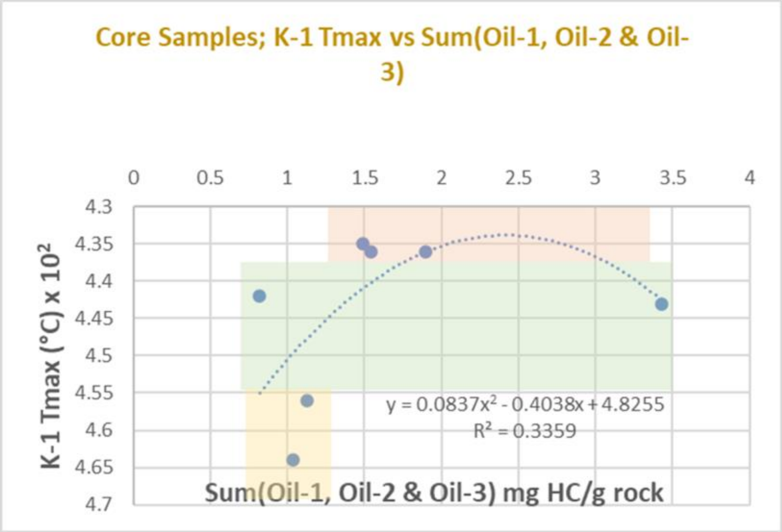

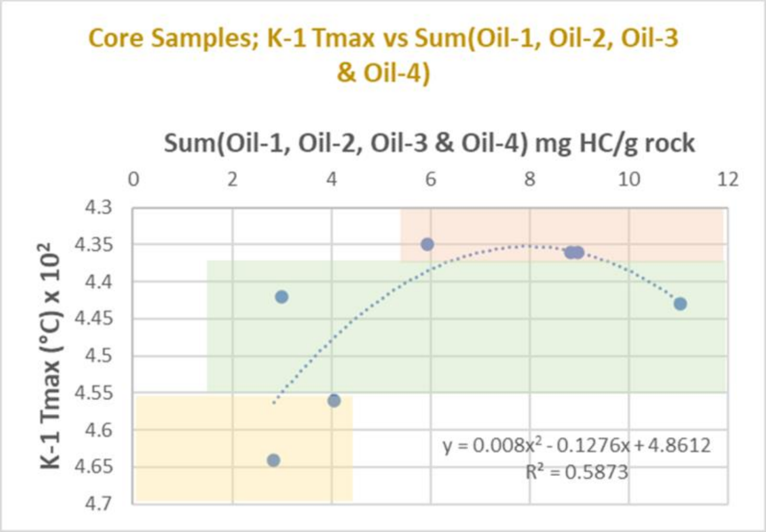

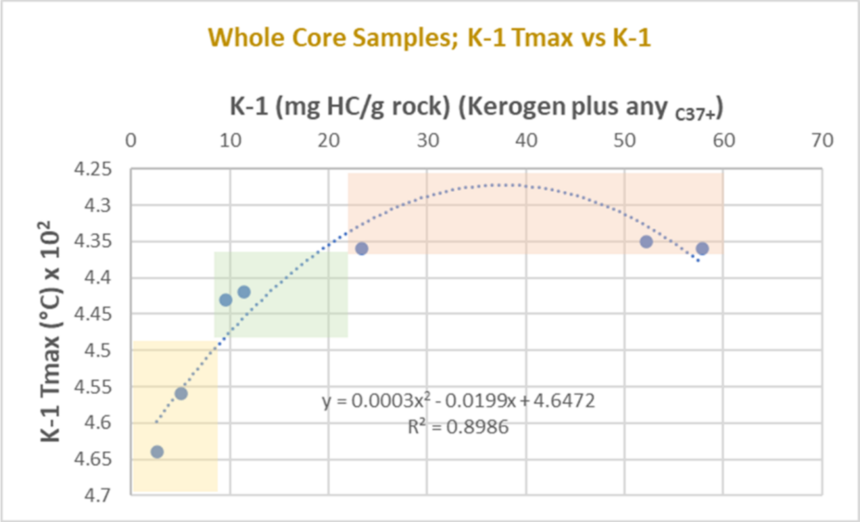

Albert Maende, Brian Horsfield, Sascha Kuske, Brian Jarvie, Dan Jarvie, and W. David Weldon

Graphical Plots of Selected Pyrolysis Measurements against Maturity (Tmax)

Figure 3. Graphical Plots of Selected Pyrolysis Measurements against Tmax

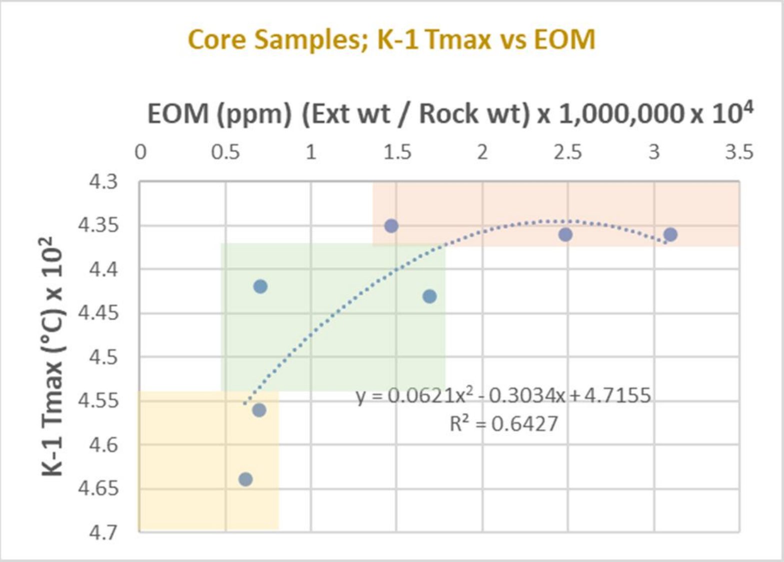

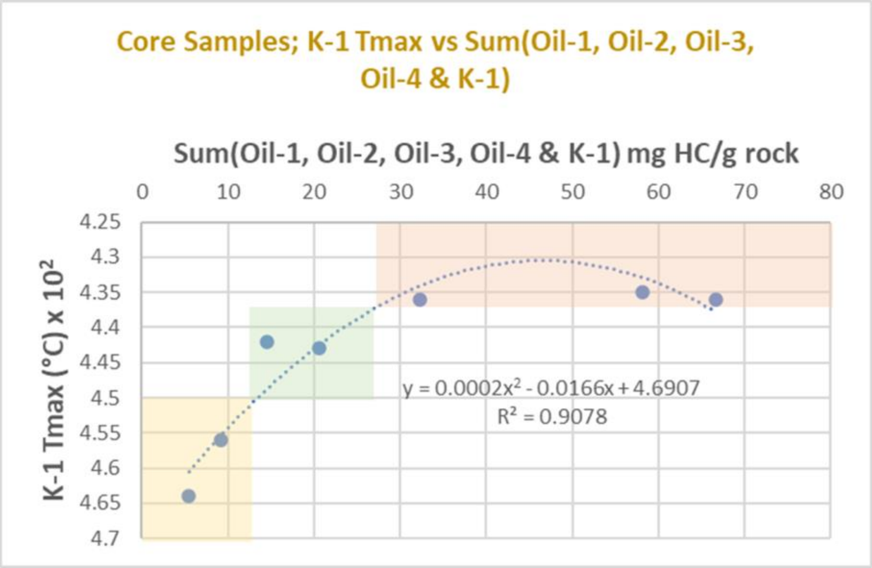

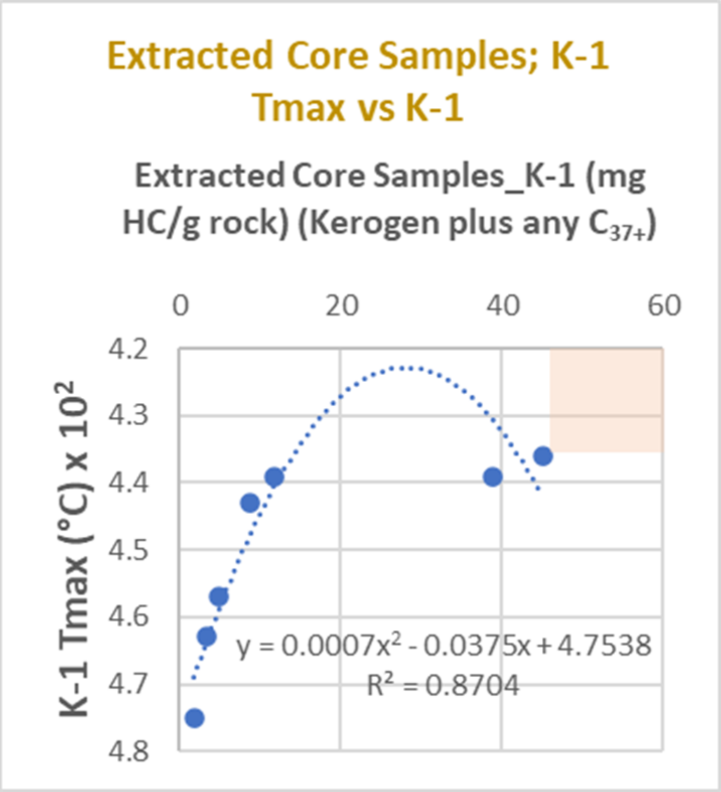

Graphical plots of selected pyrolysis measurements against Tmax (Figure 3) demonstrate that the immature, oil window and condensate to wet gas zones plot along elliptical arcs that have specified exponential equations with correlation values that range from an R^2 of 0.59 to 0.93. The highest R^2 values are in the 0.90 to 0.93 range and are those of Tmax vs S2, Tmax vs S2/S3, and K-1 Tmax vs K-1.

Albert Maende, Brian Horsfield, Sascha Kuske, Brian Jarvie, Dan Jarvie, and W. David Weldon

Ranges of Pyrolysis Parameters that Demarcate the Immature, Oil Window and Condensate to Wet Gas Zones

Maturity	Core Samples (G014171, G014174, G014177, G014180, G014183, G014185 and G014188)										Extracted Core Samples (G014171, G014174, G014177, G014180, G014183, G014185 and G014188)	
	S1 (mg HC/g rock) from Tmax vs S1	EOM (ppm) from Tmax vs EOM	S2/S3 from Tmax vs S2/S3	Sum(S1 + S2) (mg HC/g rock) from Tmax vs Sum(S1 + S2)	S2 (mg HC/g rock) from Tmax vs S2	K-1 Tmax (°C) from K-1 Tmax vs Sum(Oil-1, Oil-2 & Oil-3)	K-1 Tmax (°C) from K-1 Tmax vs Sum(Oil-1, Oil-2, Oil-3 & Oil-4)	K-1 (mg HC/g rock) from K-1 Tmax vs K-1	K-1 (mg HC/g rock) from K-1 Tmax vs EOM	K-1 (mg HC/g rock) from K-1 Tmax vs Sum(Oil-1, Oil-2, Oil-3, Oil-4 & K-1)	S2 (mg HC/g rock) from Tmax vs S2	K-1 (mg HC/g rock) from K-1 Tmax vs K-1
Immature (< 435 °C Tmax)	3.5 - 10	1.3 - 4	5 to 15	25 - 80	23 to 70	1.2 - 3.4	5.5 - 12	21 - 60	1.4 to 3.5	27 - 80	27 to 50	48 - 60
Oil Window (435 °C - 455 °C Tmax)	2 to 10	0.5 - 1.8	2.5 to 5	10 to 25	10 to 23	0.7 - 3.5	1.5 - 12	9 to 21	0.5 - 1.8	11 to 27	7 to 46	5 to 48
Condensate to Wet Gas (455 °C - 475 °C Tmax)	0 - 3.5	0 - 0.8	0 to 2.5	0 to 10	0 to 10	0.7 - 1.2	0 - 4.3	0 to 9	0.5 - 0.8	0 - 11	0 to 8	0 to 5

Table 2. Summary of the Various Ranges of Pyrolysis Parameters that Demarcate the Immature, Oil Window and Condensate to Wet Gas Zones

Albert Maende, Brian Horsfield, Sascha Kuske, Brian Jarvie, Dan Jarvie, and W. David Weldon

Comparison of Pyrolysis and Maturity Measurements of Core and Extracted Core Samples that were analyzed using Gas Chromatography (GC) and for which Evaporative Loss was Determined

Sample ID	Sample Type	S1 (mg HC/g rock)	S2 (mg HC/g rock)	S3 (mg CO2/g rock)	Tmax (°C)
G014171	Core / Extracted Core	5.3 / 0.16	25.55 / 10.78	0.48 / 0.27	436 / 440
G014174	Core / Extracted Core	2.23 / 0.20	12.17 / 9.27	0.34 / 0.30	442 / 443
G014177	Core / Extracted Core	2.82 / 0.23	5.46 / 3.10	0.24 / 0.31	458 / 465
G014180	Core / Extracted Core	2.19 / 0.25	2.91 / 1.69	0.29 / 0.26	465 / 476
G014183	Core / Extracted Core	8.33 / 0.31	11.99 / 5.00	0.41 / 0.42	443 / 458
G014185	Core / Extracted Core	6.68 / 0.13	58.08 / 39.16	0.45 / 0.31	434 / 440
G014188	Core / Extracted Core	3.94 / 0.13	52.47 / 43.87	0.42 / 0.25	435 / 437

Albert Maende, Brian Horsfield, Sascha Kuske, Brian Jarvie, Dan Jarvie, and W. David Weldon

Gas Chromatography (GC) Fingerprints of the Extracts of the Seven Core Samples that were Analyzed

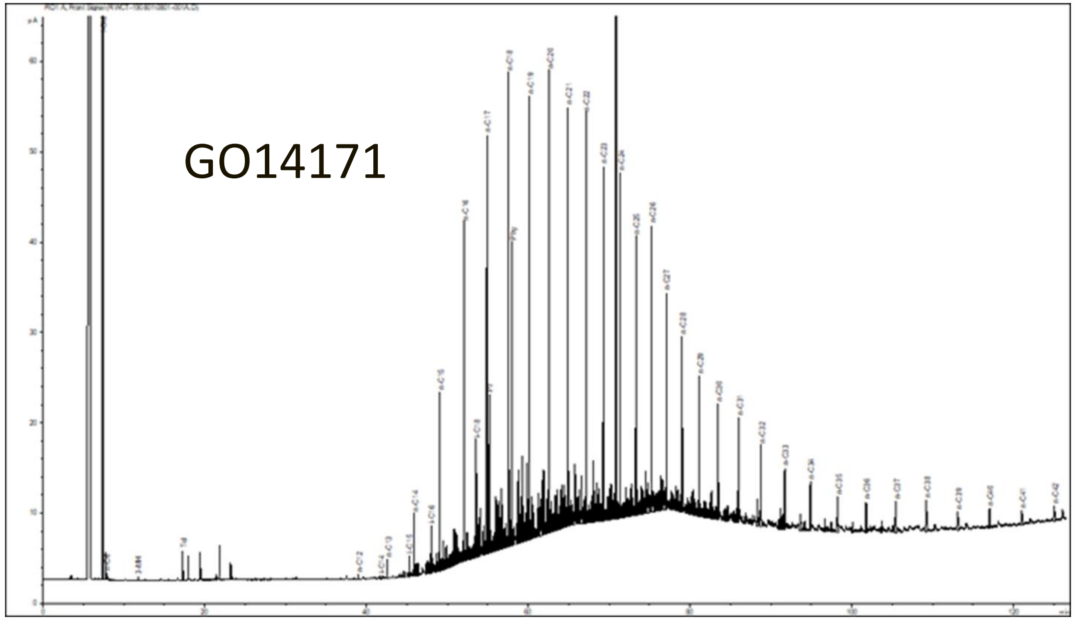

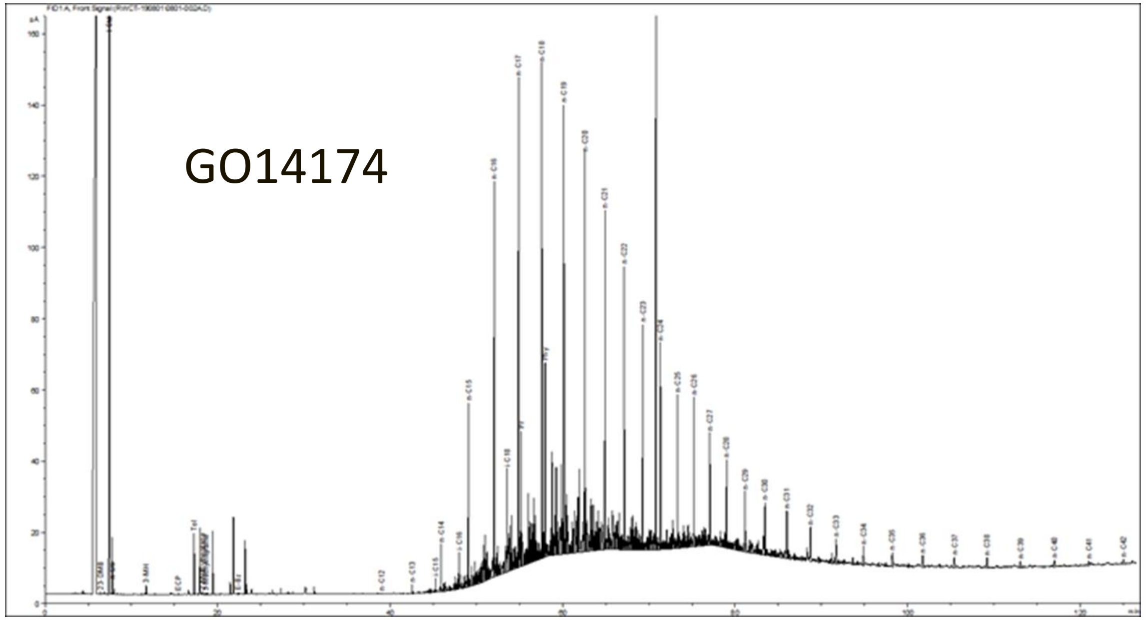

Sample ID	Sample Type	S1 (mg HC/g rock)	S2 (mg HC/g rock)	S3 (mg CO2/g rock)	Tmax (°C)
G014171	Core / Extracted Core	5.3 / 0.16	25.55 / 10.78	0.48 / 0.27	436 / 440
G014174	Core / Extracted Core	2.23 / 0.20	12.17 / 9.27	0.34 / 0.30	442 / 443
G014177	Core / Extracted Core	2.82 / 0.23	5.46 / 3.10	0.24 / 0.31	458 / 465
G014180	Core / Extracted Core	2.19 / 0.25	2.91 / 1.69	0.29 / 0.26	465 / 476
G014183	Core / Extracted Core	8.33 / 0.31	11.99 / 5.00	0.41 / 0.42	443 / 458
G014185	Core / Extracted Core	6.68 / 0.13	58.08 / 39.16	0.45 / 0.31	434 / 440
G014188	Core / Extracted Core	3.94 / 0.13	52.47 / 43.87	0.42 / 0.25	435 / 437

Albert Maende, Brian Horsfield, Sascha Kuske, Brian Jarvie, Dan Jarvie, and W. David Weldon

Gas Chromatography (GC) Fingerprints of the Extracts of the Seven Core Samples that were Analyzed and Restored Yields

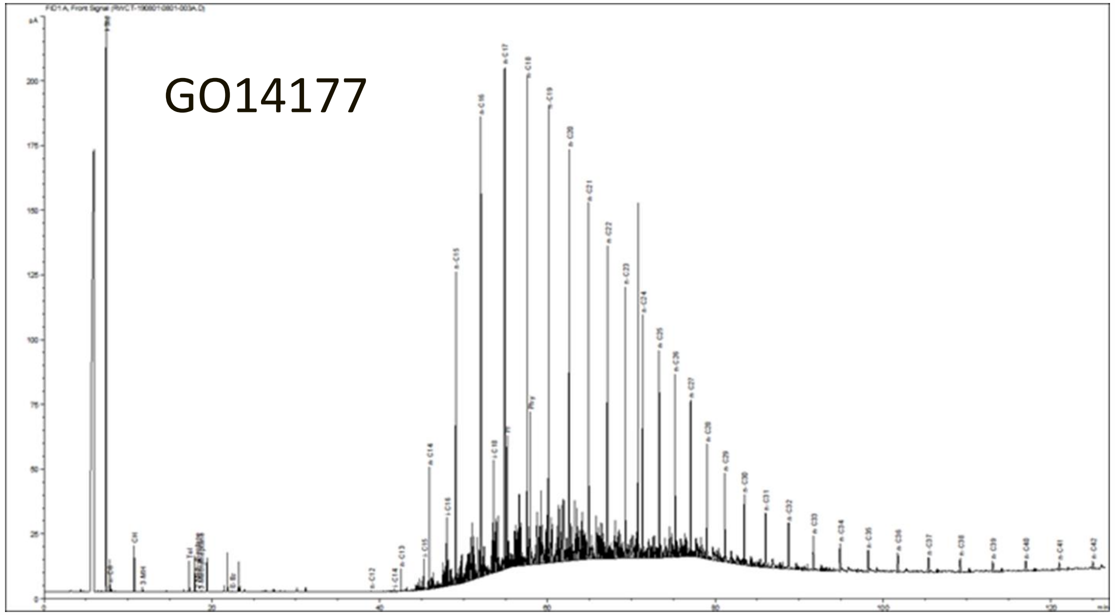

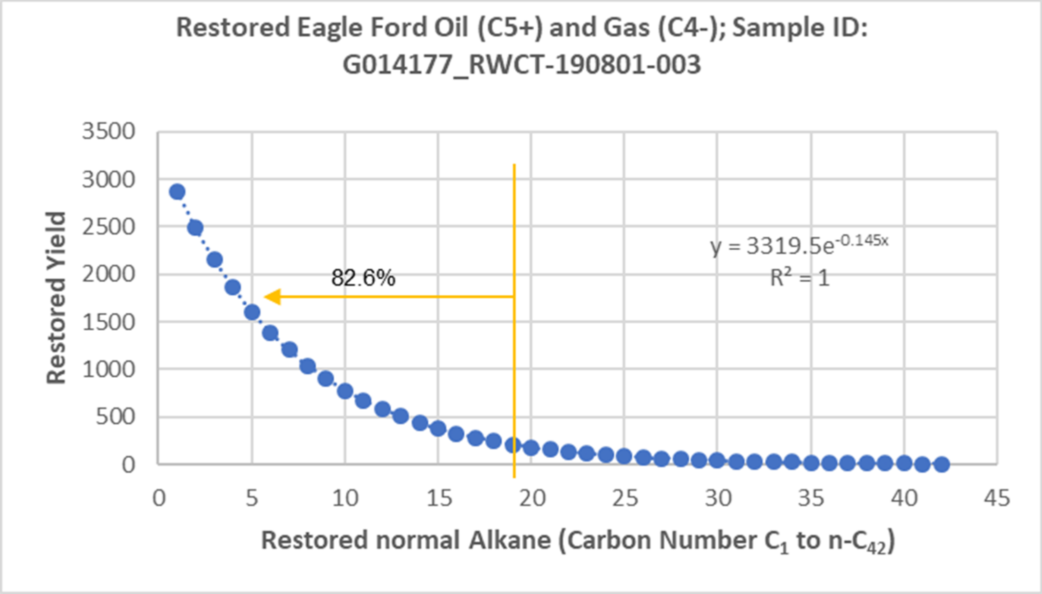

Sample ID	Sample Type	S1 (mg HC/g rock)	S2 (mg HC/g rock)	S3 (mg CO2/g rock)	Tmax (°C)
G014171	Core / Extracted Core	5.3 / 0.16	25.55 / 10.78	0.48 / 0.27	436 / 440
G014174	Core / Extracted Core	2.23 / 0.20	12.17 / 9.27	0.34 / 0.30	442 / 443
G014177	Core / Extracted Core	2.82 / 0.23	5.46 / 3.10	0.24 / 0.31	458 / 465
G014180	Core / Extracted Core	2.19 / 0.25	2.91 / 1.69	0.29 / 0.26	465 / 476
G014183	Core / Extracted Core	8.33 / 0.31	11.99 / 5.00	0.41 / 0.42	443 / 458
G014185	Core / Extracted Core	6.68 / 0.13	58.08 / 39.16	0.45 / 0.31	434 / 440
G014188	Core / Extracted Core	3.94 / 0.13	52.47 / 43.87	0.42 / 0.25	435 / 437

Samples G014177, G014180 and G014183 whose Tmax values are 458, 465 and 443 respectively, have evaporative losses of 82.6% for nC_{19-}, 83.7% for nC_{19-} and 84.2% for nC_{20-} respectively (Table 4).

Sample ID	Core_Tmax (°C)	Evaporative Loss
G014177	458	82.6%_nC_{19-}
G014180	465	83.7%_nC_{19-}
G014183	443	84.2%_nC_{20-}

Albert Maende, Brian Horsfield, Sascha Kuske, Brian Jarvie, Dan Jarvie, and W. David Weldon

Gas Chromatography (GC) Fingerprints of the Extracts of the Seven Core Samples that were Analyzed and Restored Yields

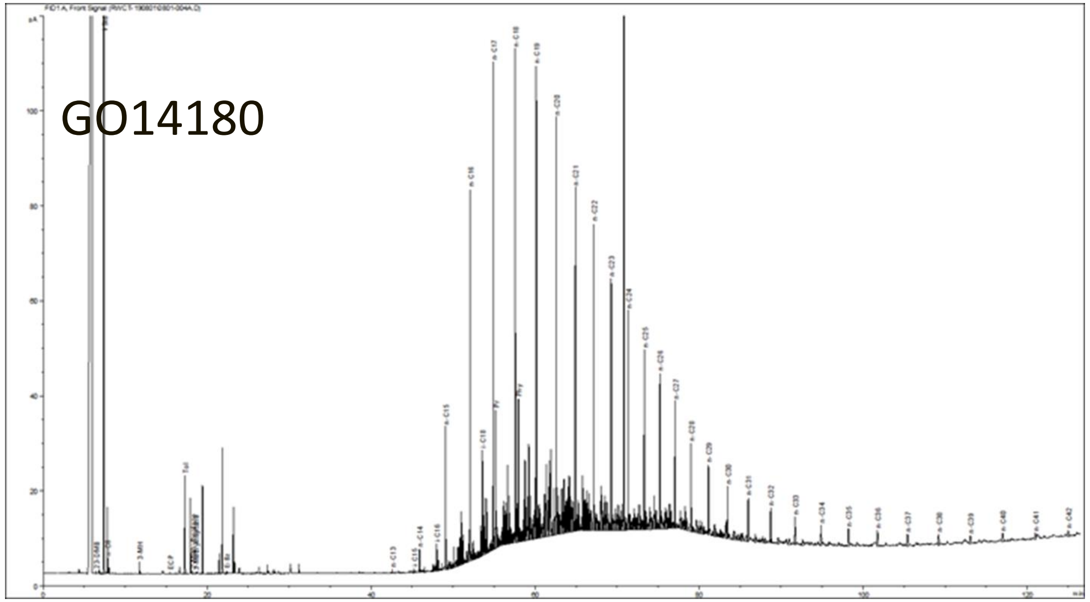

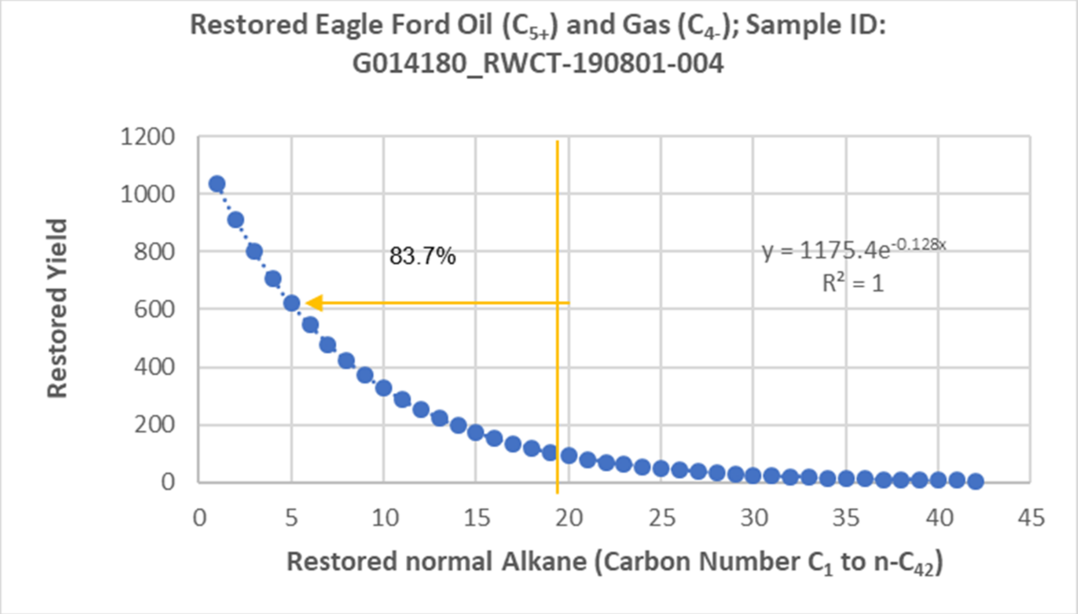

Sample ID	Sample Type	S1 (mg HC/g rock)	S2 (mg HC/g rock)	S3 (mg CO2/g rock)	Tmax (°C)
G014171	Core / Extracted Core	5.3 / 0.16	25.55 / 10.78	0.48 / 0.27	436 / 440
G014174	Core / Extracted Core	2.23 / 0.20	12.17 / 9.27	0.34 / 0.30	442 / 443
G014177	Core / Extracted Core	2.82 / 0.23	5.46 / 3.10	0.24 / 0.31	458 / 465
G014180	Core / Extracted Core	2.19 / 0.25	2.91 / 1.69	0.29 / 0.26	465 / 476
G014183	Core / Extracted Core	8.33 / 0.31	11.99 / 5.00	0.41 / 0.42	443 / 458
G014185	Core / Extracted Core	6.68 / 0.13	58.08 / 39.16	0.45 / 0.31	434 / 440
G014188	Core / Extracted Core	3.94 / 0.13	52.47 / 43.87	0.42 / 0.25	435 / 437

Samples G014177, G014180 and G014183 whose Tmax values are 458, 465 and 443 respectively, have evaporative losses of 82.6% for nC_{19-}, 83.7% for nC_{19-} and 84.2% for nC_{20-} respectively (Table 4).

Sample ID	Core_Tmax (°C)	Evaporative Loss
G014177	458	82.6%_nC_{19-}
G014180	465	83.7%_nC_{19-}
G014183	443	84.2%_nC_{20-}

Albert Maende, Brian Horsfield, Sascha Kuske, Brian Jarvie, Dan Jarvie, and W. David Weldon

ACE 2020 7-10 JUNE HOUSTON
INCORPORATING THE SEPM ANNUAL MEETING
AAPG ANNUAL CONVENTION & EXHIBITION

Gas Chromatography (GC) Fingerprints of the Extracts of the Seven Core Samples that were Analyzed and Restored Yields

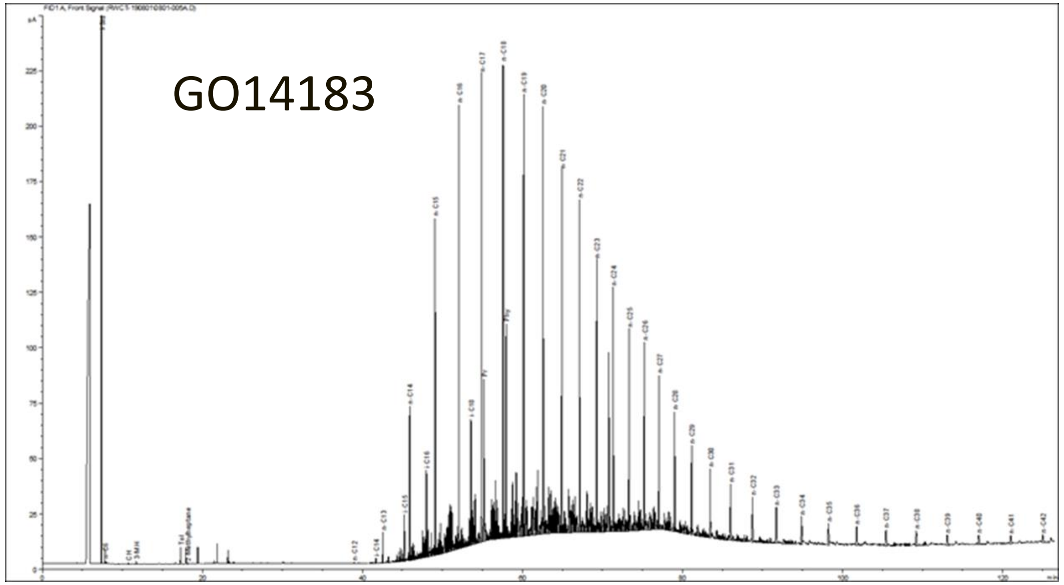

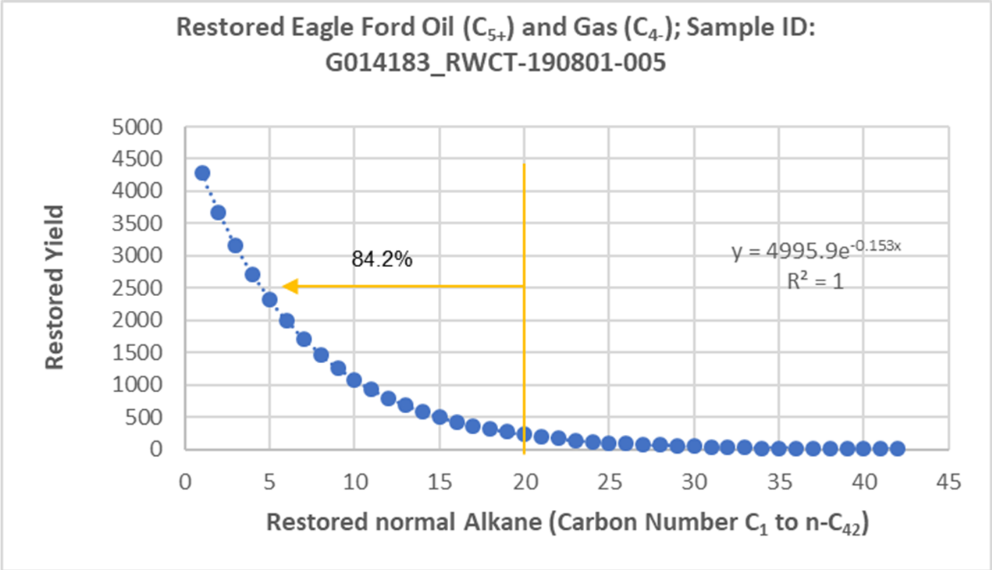

Sample ID	Sample Type	S1 (mg HC/g rock)	S2 (mg HC/g rock)	S3 (mg CO2/g rock)	Tmax (°C)
G014171	Core / Extracted Core	5.3 / 0.16	25.55 / 10.78	0.48 / 0.27	436 / 440
G014174	Core / Extracted Core	2.23 / 0.20	12.17 / 9.27	0.34 / 0.30	442 / 443
G014177	Core / Extracted Core	2.82 / 0.23	5.46 / 3.10	0.24 / 0.31	458 / 465
G014180	Core / Extracted Core	2.19 / 0.25	2.91 / 1.69	0.29 / 0.26	465 / 476
G014183	Core / Extracted Core	8.33 / 0.31	11.99 / 5.00	0.41 / 0.42	443 / 458
G014185	Core / Extracted Core	6.68 / 0.13	58.08 / 39.16	0.45 / 0.31	434 / 440
G014188	Core / Extracted Core	3.94 / 0.13	52.47 / 43.87	0.42 / 0.25	435 / 437

Samples G014177, G014180 and G014183 whose Tmax values are 458, 465 and 443 respectively, have evaporative losses of 82.6% for nC_{19-}, 83.7% for nC_{19-} and 84.2% for nC_{20-} respectively (Table 4).

Sample ID	Core_Tmax (°C)	Evaporative Loss
G014177	458	82.6%_nC_{19-}
G014180	465	83.7%_nC_{19-}
G014183	443	84.2%_nC_{20-}

Albert Maende, Brian Horsfield, Sascha Kuske, Brian Jarvie, Dan Jarvie, and W. David Weldon

Gas Chromatography (GC) Fingerprints of the Extracts of the Seven Core Samples that were Analyzed

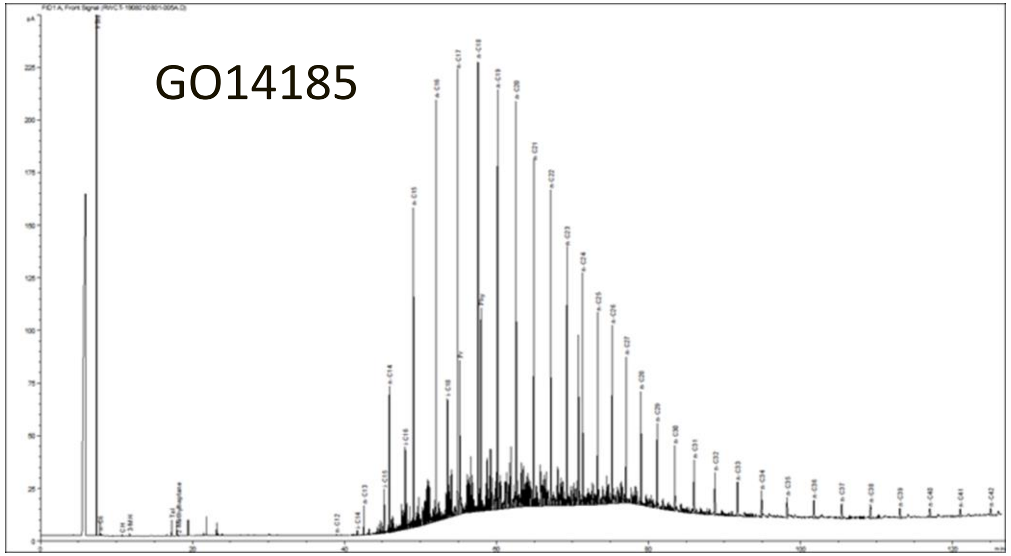

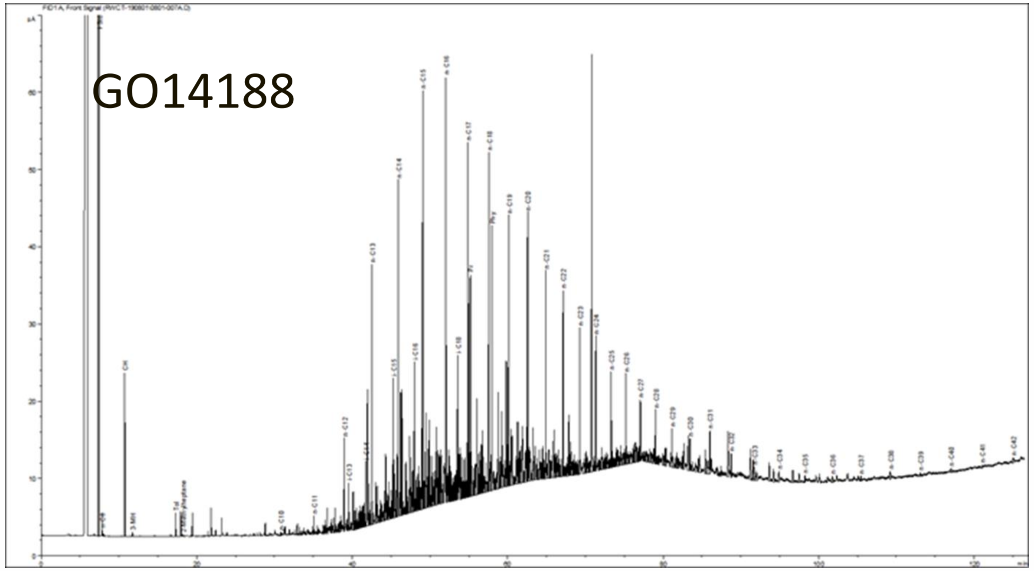

Sample ID	Sample Type	S1 (mg HC/g rock)	S2 (mg HC/g rock)	S3 (mg CO2/g rock)	Tmax (°C)
G014171	Core / Extracted Core	5.3 / 0.16	25.55 / 10.78	0.48 / 0.27	436 / 440
G014174	Core / Extracted Core	2.23 / 0.20	12.17 / 9.27	0.34 / 0.30	442 / 443
G014177	Core / Extracted Core	2.82 / 0.23	5.46 / 3.10	0.24 / 0.31	458 / 465
G014180	Core / Extracted Core	2.19 / 0.25	2.91 / 1.69	0.29 / 0.26	465 / 476
G014183	Core / Extracted Core	8.33 / 0.31	11.99 / 5.00	0.41 / 0.42	443 / 458
G014185	Core / Extracted Core	6.68 / 0.13	58.08 / 39.16	0.45 / 0.31	434 / 440
G014188	Core / Extracted Core	3.94 / 0.13	52.47 / 43.87	0.42 / 0.25	435 / 437

Figure 4 shows the gas chromatography (GC) fingerprints of the extracts of the seven core samples. Samples G014177, G014180 and G014183 whose Tmax values are 458, 465 and 443 respectively, have evaporative losses of 82.6% for nC_{19-}, 83.7% for nC_{19-} and 84.2% for nC_{20-} respectively

Albert Maende, Brian Horsfield, Sascha Kuske, Brian Jarvie, Dan Jarvie, and W. David Weldon

Pyrolysis Attributes of the Shale Prospectivity Tool

As a result of this study, the Shale Prospectivity Tool has been developed.

The objective of the Shale Prospectivity Tool is to utilize Six Pyrolysis Attributes to Predict the Occurrence of Producible Hydrocarbons and in addition, also map Structures.

The six pyrolysis attributes are determined through conversion of two Classical Pyrolysis rock measurements and four HAWK-PAM rock measurement's mg HC/g rock (milligram hydrocarbons per gram rock), values to their respective organic carbon using the assumption that 85% of hydrocarbons content in petroleum is organic carbon.

These values are then normalized to either their respective TOC (Total Organic Carbon) or Extractable Organic Matter (EOM) measurements.

Albert Maende, Brian Horsfield, Sascha Kuske, Brian Jarvie, Dan Jarvie, and W. David Weldon

Shale Prospectivity Tool

Definitions of Pyrolysis Attributes of the Shale Prospectivity Tool

The Six Pyrolysis Attributes of the Shale Prospectivity Tool are defined as shown below:

- Pyrolysis Attribute 1: - Classical Pyrolysis' S1 organic carbon content in hydrocarbons normalized to either EOM or TOC. i.e., S1*C in HCs/EOM or TOC

Pyrolysis Attributes 2, 3, 4 and 5 are all derived from HAWK-PAM measurements:

- Pyrolysis Attribute 2: - Oil4 (C_{20}-C_{36})*C in HCs /EOM or TOC

- Pyrolysis Attribute 3: - Sum of Oil1, Oil2, & Oil3 (C_4-C_{19})*C in HCs/EOM or TOC

- Pyrolysis Attribute 4: - Sum of Oil1, Oil2, Oil3 & Oil4 (C_4-C_{36})*C in HCs/ EOM or TOC

- Pyrolysis Attribute 5 is the Mobility Index: - Sum(Oil1, Oil2 & Oil3)/Sum(Oil1, Oil2, Oil3 & Oil4) (C_4 - C_{19}/C_4 - C_{36})

- Pyrolysis Attribute 6: - Classical Pyrolysis' S2 kerogen pyrolyzed hydrocarbons normalized to either EOM or TOC. i.e., S2*C in HCs/EOM or TOC

Albert Maende, Brian Horsfield, Sascha Kuske, Brian Jarvie, Dan Jarvie, and W. David Weldon

Cut-off Values of Pyrolysis Attributes of the Shale Prospectivity Tool for Determination of Producible Oil Zones

Each of these five pyrolysis attributes has been assigned a cut-off value that it needs to either equal or exceed in order for it to be a candidate to be utilized in identifying a producible oil zone. An analyzed sample that has at least three of these pyrolysis attributes either equating or exceeding the cut-off value is considered to be indicative of a producible oil zone. Table 5 and Figure 5 show that all the seven core samples fulfill the Shale Prospectivity Tool's conditions for being identified as being in a producible oil zone. However it is only the G014180 core of Tmax 465 °C (K-1 Tmax 464 °C) that equates or exceeds the Mobility Index cut-off value.

Table 5. Pyrolysis Attributes of the Shale Prospectivity Tool

Sample Type	Sample ID	S1*C in HCs/EOM; Pyrolysis Attribute 1_0.1 as cut off	Oil4 (C_{20}-C_{36})*C in HCs /EOM; Pyrolysis Atrribute 2_0.05 as cut off	Sum of Oil1, Oil2, & Oil3 (C_4-C_{19})*C in HCs/EOM; Pyrolysis Attribute 3_0.05 as cut off	Sum of Oil1, Oil2, Oil3 & Oil4 (C_4-C_{36})*C in HCs/EOM; Pyrolysis Atrribute 4_0.1 as cut off	Mobility Index; Sum(Oil1, Oil2 & Oil3)/Sum(Oil1, Oil2, Oil3 & Oil4) (C_4 - C_{19}/C_4 - C_{36}); Pyrolysis Attribute 5_0.35 as cut off
Core	G014171	0.18	0.25	0.05	0.31	0.17
Core	G014174	0.27	0.27	0.10	0.36	0.27
Core	G014177	0.34	0.36	0.14	0.50	0.28
Core	G014180	0.30	0.25	0.14	0.39	0.37
Core	G014183	0.42	0.38	0.17	0.55	0.31
Core	G014185	0.18	0.19	0.05	0.24	0.22
Core	G014188	0.23	0.26	0.09	0.34	0.25

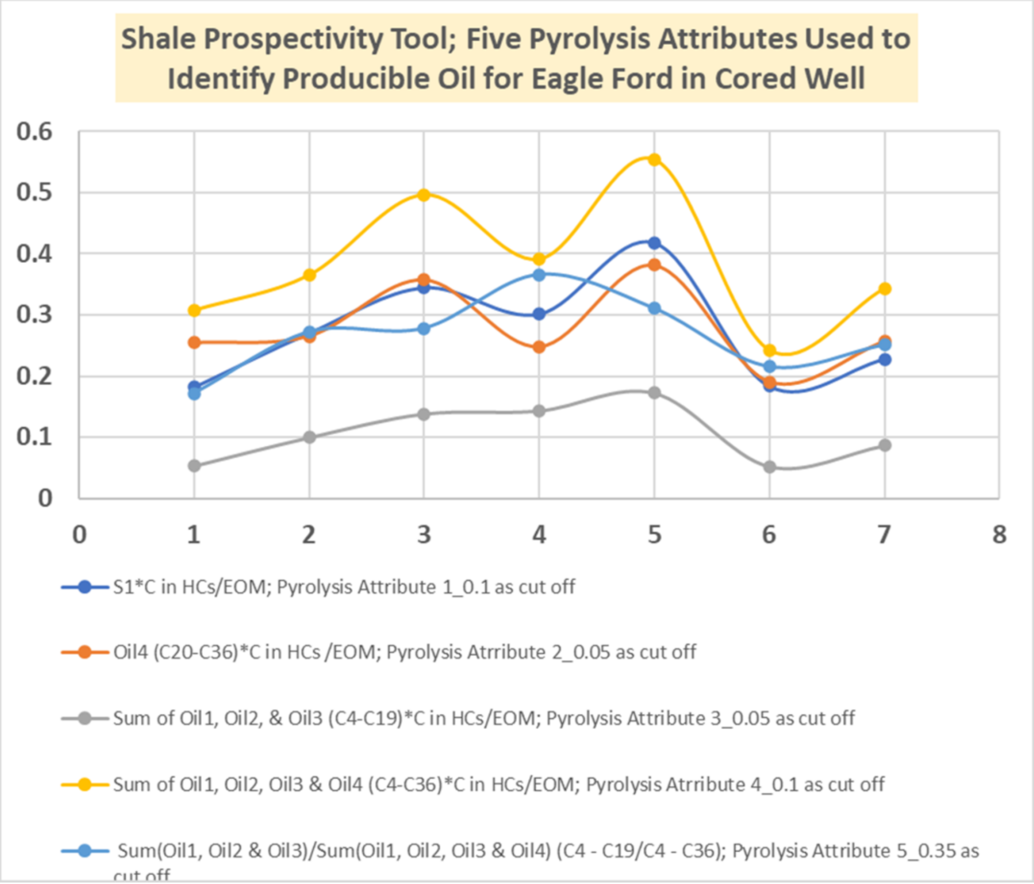

Figure 5. Graphical Plot of Five Pyrolysis Attributes of the Shale Prospectivity Tool

Albert Maende, Brian Horsfield, Sascha Kuske, Brian Jarvie, Dan Jarvie, and W. David Weldon

Shale Prospectivity Tool Mapping of the Drilled Structure

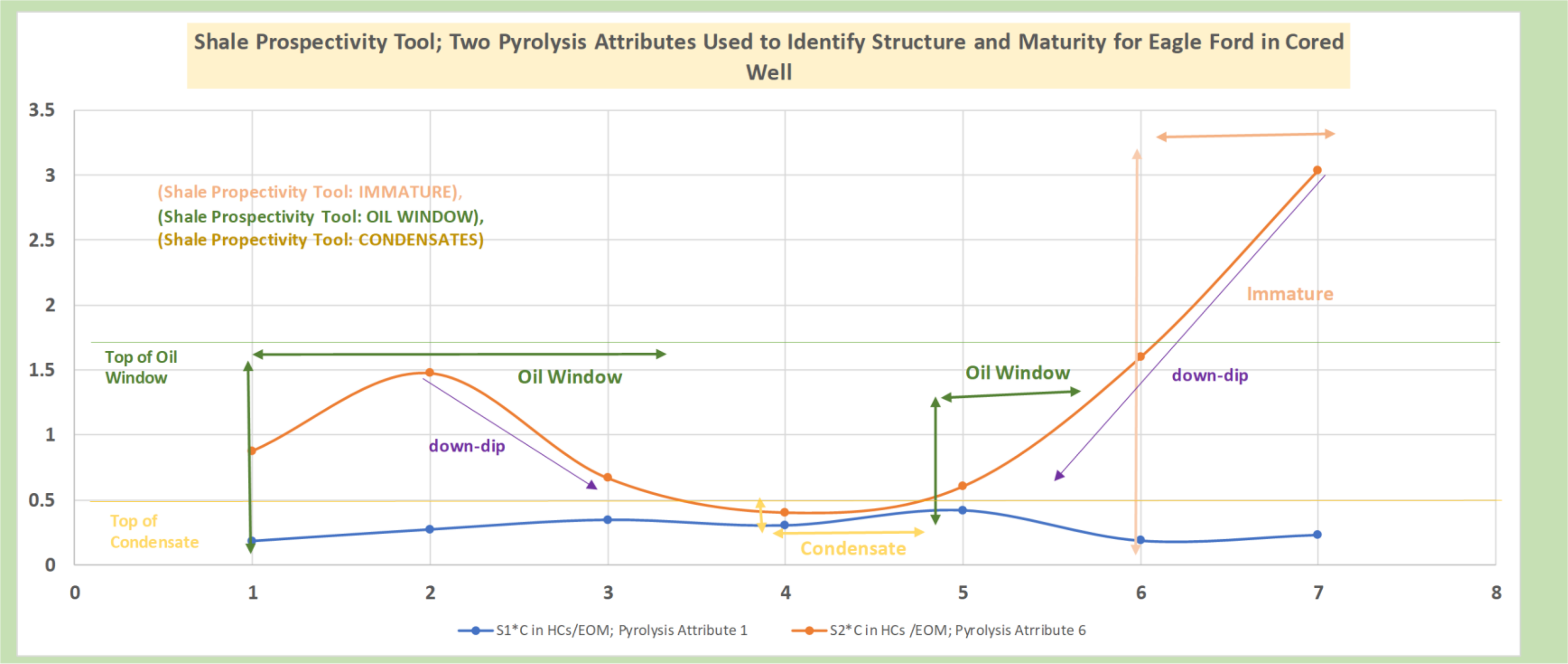

Figure 6. Two Pyrolysis Attributes of the Shale Prospectivity Tool used to Delineate Maturity Zones and Map Structure

A graphical plot of the Shale Prospectivity Tools' Pyrolysis Attribute 1 (S1*C in HCs/EOM against Pyrolysis Attribute 6 (S2*C in HCs/EOM maps the drilled structure and show the separation between these values to be widest in the immature zone, of intermediate width in the oil window and so close to each other as to be virtually touching in the condensate to wet gas zone (Figure 6). The down-dip direction can also be discerned. Kuske *et. al.*, 2019 showed that Hydrogen Index values of two of the Eagle Ford suites of samples that they analyzed, systematically varied with structural dip direction.

Albert Maende, Brian Horsfield, Sascha Kuske, Brian Jarvie, Dan Jarvie, and W. David Weldon

Conclusions

Seven core samples spanning the Eagle Ford Formation's early mature, oil window and condensate/wet gas zones were analyzed both as whole rock and extracted rock, whereby, six pyrolysis attributes that can assist in predicting producible hydrocarbon in unconventional formations and also map structures were identified and collectively labelled as "the Shale Prospectivity Tool".

The six pyrolysis attributes are determined through conversion of two Classical Pyrolysis rock measurements and four HAWK-PAM rock measurement's mg HC/g rock values to their respective organic carbon using the assumption that 85% of hydrocarbons content in petroleum is organic carbon. These values are then normalized to either their respective TOC or EOM measurements.

Conclusions

The suppression effect of ‘S2 shoulders’ on maturity was evident on four cores (those of Tmax 436, 458, 465 and 443). The “S2 shoulder” which is an overlap of the heavier oil component from S1 into S2 is quantifiable through the almost equality of the “S2 – K1” value with the “Sum(Oil-1, Oil-2, Oil-3 and Oil-4 – S1” value of the cores of Tmax 442 and 443 which are of mid oil window maturity.

Graphical plots of selected pyrolysis measurements against Tmax (Figure 3) demonstrate that the immature, oil window and condensate to wet gas zones plot along elliptical arcs that have specified exponential equations with correlation values that range from an R^2 of 0.59 to 0.93.

ACE 2020 7-10 JUNE HOUSTON INCORPORATING THE SEPM ANNUAL MEETING AAPG ANNUAL CONVENTION & EXHIBITION

Conclusions

The highest R^2 values are in the 0.90 to 0.93 range and are those of Tmax vs S2, Tmax vs S2/S3, and K-1 Tmax vs K-1. Samples G014177, G014180 and G014183 whose Tmax values are 458, 465 and 443 respectively, have evaporative losses of 82.6% for nC_{19-}, 83.7% for nC_{19-} and 84.2% for nC_{20-} respectively.

Classical Pyrolysis and **HAWK-PAM** measurements, however, do not enable the discrimination of producible hydrocarbons because of the presence of sorbed oil which is highest in early mature cores. Conversion of mg HC/g rock measurements to their respective organic carbon using the assumption that 85% of hydrocarbons content in petroleum is organic carbon, together with conversion of the quantified extracted organic matter (EOM) from ppm to weight % enabled the identification of a new set of pyrolysis attributes, which collectively are referred to as the Shale Prospectivity Tool.

An analyzed sample that has at least three of the Shale Prospectivity Tools' pyrolysis attributes either equating or exceeding the cut-off value is considered to be indicative of a producible oil zone.

Albert Maende, Brian Horsfield, Sascha Kuske, Brian Jarvie, Dan Jarvie, and W. David Weldon

Conclusions

All the Eagle Ford Formation's seven analyzed core samples, fulfill the Shale Prospectivity Tool's conditions for being identified as being in a producible oil zone. However it is only the G014180 core of Tmax 465 °C (K-1 Tmax 464 °C) that equates or exceeds the Mobility Index pyrolysis attribute cut-off value.

A graphical plot of the Shale Prospectivity Tools' Pyrolysis Attribute 1 (S1*C in HCs/EOM) against Pyrolysis Attribute 6 (S2*C in HCs/EOM) maps the drilled structure and show, the separation between these values to be widest in the immature zone, of intermediate width in the oil window and so close to each other as to be virtually touching in the condensate to wet gas zone.

The Shale Prospectivity Tools' Pyrolysis Attributes enable ranking of predicted producible hydrocarbons, with the highest to lowest values in each of the attributes, corresponding to highest to lowest producible hydrocarbon contents. Determination of these pyrolysis attributes for a producing interval can provide calibration for predicting similar production.

Albert Maende, Brian Horsfield, Sascha Kuske, Brian Jarvie, Dan Jarvie, and W. David Weldon

Acknowledgements and References

Acknowledgements

We are grateful to Wildcat Technologies and German Research Centre for Geosciences for allowing the publication of this study. We also wish to thank AAPG for giving us this opportunity to make our presentation.

References

EIA, 2014, Updates to the EIA Eagle Ford Play Maps, https://www.eia.gov/maps/pdf/eagleford1014.pdf accessed on April 29th, 2020.

Gorynski, K. E., M. H. Tobey, D. A. Enriquez, T. M. Smagala, J. L. Dreger and R. E. Newhart, 2019, Quantification and Characterization of Hydrocarbon-Filled Porosity in Oil-Rich Shales Using Integrated Thermal Extraction, Pyrolysis and Solvent Extraction, AAPG Bulletin, v. 103, No. 3 (March 2019), pp. 723-744.

Jarvie, D. M., B. M. Jarvie, D. Weldon and A. Maende, 2015, Geochemical Assessment of in situ Petroleum in Unconventional Resource Systems, Unconventional Resources Technology Conference (URTeC) DOI 10.15530/urtec-2015-2174325. This paper was prepared for presentation at the Unconventional Resources Technology Conference held in San Antonio, Texas, USA, 20-22 July 2015.

Jarvie, D. M., 2012, Shale Resource Systems for Oil and Gas: Part 2 – Shale Oil Resource Systems, in J. A. Breyer, ed., Shale Reservoirs – Giant Resources for the 21st Century: AAPG Memoir 97, pp. 89 – 119.

Kuske, S., B. Horsfield, J. Jweda, G. E. Michael and Y. Song, 2019, Geochemical Factors Controlling the Phase Behavior of Eagle Ford Shale Petroleum Fluids, AAPG Bulletin, v. 103, No. 4 (April 2019), pp. 835-870.

References

Maende, A., A. Pepper, D. M. Jarvie, and W. D. Weldon, 2017, Advanced Pyrolysis Data and Interpretation Methods to Identify Unconventional Reservoir Sweet Spots in Fluid Phase Saturation and Fluid Properties (API Gravity) From Drill Cuttings and Cores, Search and Discovery Article #80596 (2017), Adapted from oral presentation given at AAPG 2017 Annual Convention and Exhibition, Houston, Texas, April 2-5, 2017. http://www.searchanddiscovery.com/pdfz/documents/2017/80596maende/ndx_maende.pdf.html

Ononogbu, U., 2012, Biomarkers: Review and Application to the Eagle Ford Formation, University of Texas at Arlington.

Pepper, A., S. Perry, and L. Heister, 2019, Saturation Isn't What It Used to Be: Towards More Realistic Petroleum Fluid Saturations and Produced Fluid Compositions in Organic-Rich Unconventional Reservoirs, Unconventional Resources Technology Conference (URTeC) DOI 10.15530/urtec-2019-196. This paper was prepared for presentation at the Unconventional Resources Technology Conference held in Denver, Colorado, USA,22-24 July 2019.